

⁹⁰Y Hepatic Radioembolization: An Update on Current Practice and Recent Developments

Arthur J.A.T. Braat, Maarten L.J. Smits, Manon N.G.J.A. Braat, Andor F. van den Hoven, Jip F. Prince, Hugo W.A.M. de Jong, Maurice A.A.J. van den Bosch, and Marnix G.E.H. Lam

Department of Radiology and Nuclear Medicine, University Medical Center Utrecht, Heidelberglaan, Utrecht, The Netherlands

Learning Objectives: On successful completion of this activity, participants should be able to (1) describe the status of the current literature regarding new indications for radioembolization; (2) describe standard hepatic vascularization, identify common routes for extrahepatic depositions, and judge when “skeletalization” of hepatic arteries could be unnecessary; and (3) appraise the different methods of activity calculation and recognize the strengths and pitfalls of pretreatment and posttreatment dosimetry.

Financial Disclosure: Dr. Lam is a consultant/advisor for BTG International and a meeting participant/lecturer for SirTex Medical. The authors of this article have indicated no other relevant relationships that could be perceived as a real or apparent conflict of interest.

CME Credit: SNMMI is accredited by the Accreditation Council for Continuing Medical Education (ACCME) to sponsor continuing education for physicians. SNMMI designates each *JNM* continuing education article for a maximum of 2.0 AMA PRA Category 1 Credits. Physicians should claim only credit commensurate with the extent of their participation in the activity. For CE credit, SAM, and other credit types, participants can access this activity through the SNMMI website (<http://www.snmmilearningcenter.org>) through July 2018.

Radioembolization is an established treatment modality that has been subjected to many improvements over the last decade. Developments are occurring at a high pace, affecting patient selection and treatment. The aim of this review is therefore to provide an overview of current practice, with a focus on recent developments in the field of radioembolization. Several practical issues and recommendations in the application of radioembolization will be discussed, ranging from patient selection to treatment response and future applications.

Key Words: radioembolization; dosimetry; liver malignancies; hepatic vasculature; ⁹⁰Y

J Nucl Med 2015; 56:1079–1087

DOI: 10.2967/jnumed.115.157446

As an established treatment modality for chemoresistant, unresectable hepatic malignancies, radioembolization has expanded its applications in recent years. Radioembolization is based on the administration of ⁹⁰Y-loaded microspheres in the arterial vasculature of the liver. Currently, two types of microspheres are Food and Drug Administration–approved and commercially available: resin microspheres (SIR-spheres; SirTex Medical) and glass microspheres (TheraSpheres; BTG International Ltd.). Because of preferential arterial flow, the microspheres occlude small tumor arterioles, thus selectively irradiating tumors. This review aims to give an overview of current developments in the field of ⁹⁰Y hepatic radioembolization.

PATIENT SELECTION

Currently, radioembolization is indicated mainly in a palliative setting for primary and secondary hepatic malignancies, only when

other (minimal) invasive or chemotherapeutic treatments have failed. Work-up for radioembolization includes clinical status, hematologic and biochemical status, anatomic assessment with CT/MR imaging, and, when appropriate, molecular imaging with SPECT/CT or PET/CT. The indications and contraindications (Table 1) need to be assessed by a multidisciplinary team (1,2). Unlike many treatment modalities, age is not a contraindication for radioembolization and has not been shown to alter prognosis (3,4).

Sufficient liver function is of primary importance and is regarded as the greatest limitation (Child–Pugh score \leq B7). Before considering radioembolization (when sufficient liver function is present), portal venous integrity, prior surgical treatments, and prior liver-directed treatments need to be evaluated. Compromised portal venous integrity is most commonly caused by a portal vein tumor thrombus (PVT), resulting in a greater dependence of the liver parenchyma on its arterial supply (5). Theoretically, after embolization a compromised portal circulation could jeopardize liver function because of ischemia or infarction, induced by the arterial occlusion. However, radioembolization has a low embolic effect, and most of the arterial tree remains patent after treatment (6,7). Radioembolization in the setting of PVT is therefore safe and can sometimes lead to complete portal vein revascularization, even in main PVT (8). In contrast to transarterial chemoembolization (TACE), PVT is not considered a contraindication. Radioembolization is an emerging indication in early-advanced hepatocellular carcinoma (HCC) (Barcelona Clinical Liver Cancer [BCLC] C, liver-dominant, Eastern Cooperative Oncology Group [ECOG] 1–2, PVT) (8). On the basis of current evidence, application of radioembolization in patients with a Child–Pugh score higher than B7 and main PVT should be weighed carefully, because of the limited potential survival benefit after radioembolization (4.5–5 mo in Child–Pugh B patients and 2.5 mo in Child–Pugh C patients vs. 2.7–4.0 mo in untreated patients) (9–12).

Prior surgical liver resection is no contraindication for radioembolization. However, surgical procedures involving the biliary tract may be a risk factor for infectious complications. The incidence of hepatic abscesses after radioembolization in patients with a normal biliary tree, or in the presence of a biliodigestive anastomosis, is fortunately low—less than 1% (Table 2) (13)—as

Received Mar. 12, 2015; revision accepted Apr. 25, 2015.

For correspondence or reprints contact: Arthur J.A.T. Braat, Heidelberglaan 100, 3584 CX Utrecht, The Netherlands.

E-mail: a.j.a.t.braat@umcutrecht.nl

Published online May 7, 2015.

COPYRIGHT © 2015 by the Society of Nuclear Medicine and Molecular Imaging, Inc.

TABLE 1
Common Indications and Relative and Absolute Contraindications for Radioembolization

Indication	Relative contraindications	Absolute contraindications
Disease not amenable to surgical resection, liver transplantation, or curative ablative therapies	Portal vein thrombosis of main branch	Extensive and untreated portal hypertension
Disease not amenable to or refractory to chemotherapeutic alternatives, or patient not willing to receive these alternatives	Abnormalities of bile ducts or stents; exceptions: papillotomy and cholecystectomy	Life expectancy < 3 mo
Compensated or early decompensated liver cirrhosis (Child–Pugh ≤ B7)	Serum bilirubin > 34.2 μmol/L (2 mg/dL)	Active hepatitis
Performance state (ECOG) ≤ 2	Leukocytes < 2 × 10 ⁹ /L or platelet count < 60 × 10 ⁹ /L	Extrahepatic deposition of ^{99m} Tc-MAA on SPECT/CT or contrast on C-arm CT
Liver-only or liver-dominant disease	Glomerular filtration rate < 35 mL/min	Unacceptable lung shunt*
Preoperative indications	INR > 1.5	

*Lung absorbed dose < 30 Gy in single session and < 50 Gy in multiple sessions.
INR = Internationalized Normalized Ratio.

opposed to less than 5% in the general TACE population and 48%–86% after TACE in the presence of a bilidigestive anastomosis (14,15). An aggressive prophylactic antibiotic regimen is therefore not advised (16,17). Radioembolization in the presence of a bilidigestive anastomosis seems safe but needs further attention, as liver abscesses after TACE show a high mortality rate of 11%–50% (15,18). Currently, a bilidigestive anastomosis is considered to be a relative contraindication for radioembolization, but this view is based on the available TACE literature because there is only limited evidence for radioembolization.

HEPATIC VASCULARIZATION AND ANGIOGRAPHIC CONSIDERATIONS

The standard hepatic arterial supply originates from a celiac trifurcation, from which the common hepatic artery arises. The common hepatic artery becomes the proper hepatic artery, after

the gastroduodenal artery has branched off. The proper hepatic artery continues toward the hilar plate, where it splits into the right and left hepatic arteries (19). Anatomic variants of the hepatic arterial vasculature are common, and correct identification of these variants is essential as it may increase the risk of extrahepatic deposition (20). Information on arterial liver vascularization derived from preprocedural liver CT–angiography or MR imaging–angiography (e.g., with an early arterial phase) is paramount for successful angiography (19,21). Anatomic variants are frequently missed in clinical practice in the absence of a thorough evaluation of the arterial vascularization on multimodality imaging. This results in unnecessary additional angiography procedures and incomplete radioembolization treatments.

The severity of an extrahepatic deposition of microspheres depends on the affected organ and the number of displaced microspheres, and its location depends on the culprit vessel. Previously, so-called skeletonization of the hepatic arteries was advised to avoid

TABLE 2
Current Literature on Liver Abscesses and Bilidigestive Anastomoses After Radioembolization

Study	Treatment	Total (n)	BDA (n)	Abscess incidence	Comment
Atassi (13)	Radioembolization	327	NR	0.3% of total	0.3% (1 patient with bilidigestive anastomosis)
Cholapranee (17)	Radioembolization + prophylaxes*	16	11	0%	5/16 had biliary stents
	Chemoembolization + prophylaxes*	13	5	23% of total	Not reported how many patients with liver abscess had bilidigestive anastomosis
Geisel (16)	Radioembolization	168	9	0%	
Korkmaz (78)	Radioembolization [†]	1	0	—	
Mascarenhas (18)	Radioembolization [†]	1	0	—	

*Levofloxacin, 500 mg daily, and metronidazole, 500 mg twice daily, for 2 wk. Additionally, 1,000 mg of neomycin and 1,000 mg of erythromycin 3 times on day of intervention.

[†]Case report.

BDA = number of patients with bilidigestive anastomoses; NR = not reported.

TABLE 3
The 3 Most Common Culprit Vessels (20,21,23,79,80)

Characteristic	Gastroduodenal artery	Cystic artery	Right gastric artery
Origin	Common hepatic artery	Right hepatic artery	Left hepatic artery (42%)
	Other (3%)	Other (2%)	Proper hepatic artery (40%)
			Gastroduodenal (10%)
			Right hepatic artery (4%)
			Common hepatic artery (3%)
Possible complication	Gastroduodenal ulcer	Radiation-induced cholecystitis (0%–7%)	Gastric ulcer
	Pancreatitis		
Coil embolization?	Not needed when there is (1) hepatopetal flow, (2) distal placement of microcatheter (>4–5 cm), (3) no extrahepatic contrast on C-arm CT	Not needed; microcatheter distal from origin is preferred	Not needed when there is distal placement of microcatheter (>4–5 cm), no extrahepatic contrast on C-arm CT

extrahepatic depositions (2). In recent years, however, this has been debated. Skeletonization can be quite an endeavor, and new hepatic–enteric collaterals may develop after coil embolization (22). Moreover, numerous disadvantages are related to the angiography procedure itself: increased procedure complexity, additional radiation dose, potential vessel damage, and complications of coil deployment. At present, most experienced centers try to avoid coil embolization. Significant extrahepatic depositions are found mostly within the distribution of 3 distinct side-branches (Table 3): the gastroduodenal artery, cystic artery, and right gastric artery (20,21). In a recent case series of 134 patients, 68.7% did not undergo coil embolization of either the gastroduodenal artery or right gastric artery. After radioembolization with glass microspheres, 1% developed a gastric ulcer (23). On the other hand, in a case series of 247 patients treated with resin microspheres, 3.2% developed a biopsy-proven gastroduodenal ulcer, despite skeletonization (24). Potential culprit vessels need to be assessed and coiled individually. Thus, standard rigorous occlusion of all side-branches of the hepatic arteries (e.g., skeletonization) has been abandoned (23).

If an extrahepatic deposition of activity is found on pretreatment simulation with ^{99m}Tc-macroaggregated albumin (^{99m}Tc-MAA) SPECT/CT, coil-embolizing the culprit vessel, a more distal position

of the catheter, or superselective catheterization, can provide a safe treatment procedure, rendering 91%–96% of the prior selected patients eligible for radioembolization (25,26). To avoid the need for a second pretreatment angiography procedure, the use of catheter-directed CT (e.g., C-arm cone-beam CT or hybrid angiography/CT) may prove indispensable. The culprit vessels can be identified during angiography and coil-embolized immediately (Fig. 1) (27). Additionally, C-arm CT can assess tumor coverage during the angiography procedure. Unenhanced tumor regions can be detected, often leading to identification of additional supplying arteries, preventing incomplete treatment. The C-arm CT provides the interventional radiologist with valuable feedback during the angiography procedure and affects the treatment plan in up to 52% of the patients (28).

PRETREATMENT IMAGING AND DOSIMETRY

Pretreatment simulation is currently based on ^{99m}Tc-MAA SPECT/CT for assessment of extrahepatic depositions and lung shunting. Lung shunting is caused by arteriovenous anastomoses or shunts in the liver parenchyma or tumor, potentially resulting in radiation pneumonitis after radioembolization (29,30). The highest tolerable lung shunt absorbed dose was defined as 30 Gy after a single treatment and up to 50 Gy after repeated treatments, in analogy with external-beam radiation therapy of the liver (31). The lung shunt fraction is usually calculated using the counts in a region of interest of the lungs, divided by the total counts in a region of interest of the lungs plus the liver (including tumor activity). However, this method is based on planar imaging and is operator- and institution-dependent. Overall, an absolute threshold (in Gy) is preferred over a relative one. Moreover, SPECT/CT leads to more accurate calculation of lung shunt absorbed dose than does planar imaging. Up to a 170% overestimation can occur when absorbed dose to the lung shunt is calculated on planar imaging compared with SPECT/CT imaging (31,32). Elschot et al. determined the lung shunt dose on planar

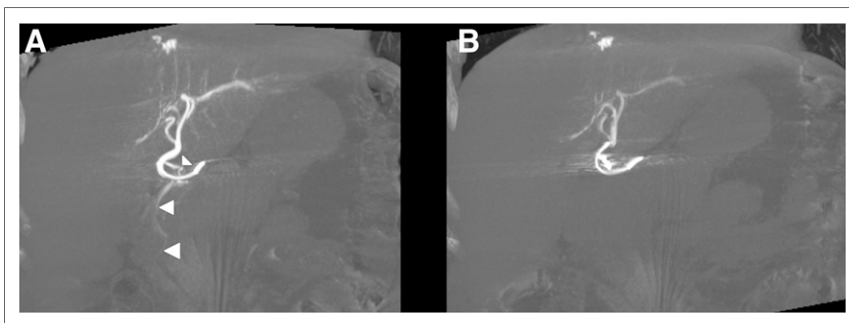


FIGURE 1. Coronal reconstructions of C-arm CT in patient before radioembolization. During angiography, catheter was positioned in proximal left hepatic artery. (A) C-arm CT illustrates arterial flow of contrast agent toward pancreatic head/duodenal region, supplied by supraduodenal artery (arrowheads), missed during digital subtraction angiography. On the basis of this additional finding, artery was occluded. (B) After coil embolization, contrast flow toward gastrointestinal tract was resolved.

TABLE 4
Pretreatment Activity Calculation Methods

Method	Activity calculation equation
Empiric (33)	Tumor load $\leq 25\%$ = 2.0 GBq whole-liver delivery, tumor load 25%–50% = 2.5 GBq whole-liver delivery, tumor load $\geq 50\%$ = 3.0 GBq whole-liver delivery
Body surface area (33)	$A(\text{GBq}) = (\text{BSA} - 0.2) + \left[\frac{\text{tumor volume}}{\text{tumor volume} + \text{liver volume}} \right]$ in which: $\text{BSA} = 0.20247 \times \text{height}(\text{m})^{0.725} \times \text{weight}(\text{kg})^{0.425}$
Partition (33)	$A(\text{GBq}) = \frac{D(\text{Gy}) \times \left(\left[\frac{1}{N} \times \text{mass}_{\text{tumor}}(\text{kg}) \right] + \text{mass}_{\text{liver}}(\text{kg}) \right)}{49,670 \times (1 - \text{lung shunt fraction})}$ in which, based on $\text{MAA SPECT/CT: T/N} = \frac{\text{Activity}_{\text{tumor}}(\text{GBq}) / \text{Mass}_{\text{tumor}}(\text{kg})}{\text{Activity}_{\text{liver}}(\text{GBq}) / \text{Mass}_{\text{liver}}(\text{kg})}$
Glass microspheres (34)	$A(\text{GBq}) = \frac{D(\text{Gy}) \times \text{mass}_{\text{liver}}(\text{kg})}{50 \times (1 - \text{lung shunt fraction})}$ with upper limit of lung shunt activity: $\text{Lung shunt fraction}(\%) \times A(\text{GBq}) = 0.61 \text{ GBq}$

imaging and SPECT/CT using $^{99\text{m}}\text{Tc}$ -MAA (150 MBq) and ^{166}Ho -microspheres (250 MBq) (32). The true mean absorbed dose based on ^{166}Ho SPECT/CT was 0.02 Gy. The absorbed dose was significantly overestimated by pretreatment planar imaging ($^{99\text{m}}\text{Tc}$ -MAA, 5.5 Gy, and ^{166}Ho , 10.4 Gy) and by $^{99\text{m}}\text{Tc}$ -MAA SPECT/CT (2.5 Gy). At present, no alternative for $^{99\text{m}}\text{Tc}$ -MAA is commercially available.

In the absence of significant extrahepatic activity, the only true dosimetric limitation left is the total absorbed radiation dose in healthy liver parenchyma, also called the nontumor dose. Little is known about the maximum tolerable nontumor dose in radioembolization. It varies between patients depending on multiple variables, including distribution of radiation within the nontumor volume. A nontumor dose limit of less than 70 Gy has been proposed (nontumor dose limit of less than 50 Gy in cirrhotic livers), although these limits seem quite arbitrarily defined and need to be confirmed in prospective studies (33). Nevertheless, pretreatment dosimetry is important to calculate the appropriate prescribed activity. Currently, 4 methods of calculating pretreatment activity are available for commercially available microspheres (Table 4) (33,34). For resin microspheres, the previously used activity calculation method was the empiric method. This method, which was based solely on tumor load, with no other patient-based factors, led to an unacceptable clinical and laboratory toxicity profile and was therefore abandoned (2,35). The second method, the body surface area method, is semiempiric and has been used safely in many clinical trials. Its main limitation is the absence of target volume in the calculation method, which can result in undertreatment (small patient with large liver) or overtreatment (large patient with small liver) (35,36). Furthermore, it does not correct for the individual intrahepatic distribution differences, calculated by the so-called tumor-to-nontumor ratio, which is to the disadvantage of patients with hyper- or hypovascular tumors. Theoretically, embedding the tumor-to-nontumor ratio in the activity calculation method for patients with hypervascular tumors will lead to a higher administered dose and higher tumor dose without compromising healthy liver tissue. The third calculation method, the so-called partition model, takes most relevant factors into account. Because the variables are acquired on $^{99\text{m}}\text{Tc}$ -MAA SPECT/CT before radioembolization, no additional procedures are needed (37,38). However, poorly defined tumors pose a problem for segmentation and quantification, and the overall complexity of the partition method renders its use less attractive in daily

practice. For radioembolization using glass microspheres, an activity calculation method is advocated without the use of a tumor-to-nontumor ratio (34). In analogy to the discussion surrounding activity calculation for resin microspheres, the partition model based on prior $^{99\text{m}}\text{Tc}$ -MAA SPECT/CT has been shown feasible for glass microspheres as well (8).

In daily practice, the body surface area method for resin microspheres and the volume-based calculation method for glass microspheres are the most commonly applied methods of calculating activity for radioembolization. Nonetheless, the partition model based on pretreatment $^{99\text{m}}\text{Tc}$ -MAA SPECT/CT should be preferred by nuclear physicians and interventional radiologists, because lesion-based dosimetry on pretreatment $^{99\text{m}}\text{Tc}$ -MAA SPECT/CT has been shown to correlate with response and survival (39–43). The aim of radioembolization is to deliver the highest possible absorbed dose to tumor cells (“tumor dose”) in order to induce apoptosis and tumor load reduction. The group of Garin et al. recently showed interesting results with the so-called partition method for treatment planning of glass microspheres. Treatment planning was based on a target tumor dose of more than 205 Gy and a nontumor dose of less than 120 Gy as calculated on $^{99\text{m}}\text{Tc}$ -MAA SPECT/CT. In 41 HCC patients with PVT (12/41 main branch), a median overall survival of 18 mo was found. Patients with a tumor dose of more than 205 Gy had significantly longer progression-free survival and overall survival (8). The rationale of tumor dose–response correlations has been supported by clinical studies in different settings (39,44). One should bear in mind, however, that partition modeling is based on $^{99\text{m}}\text{Tc}$ -MAA SPECT/CT, which is influenced by many factors, including discrepancies between $^{99\text{m}}\text{Tc}$ -MAA and $^{90\text{Y}}$ -microsphere distribution (Fig. 2). Several alternatives to $^{99\text{m}}\text{Tc}$ -MAA are currently under investigation, mainly to avoid discrepancies based on morphologic differences between $^{99\text{m}}\text{Tc}$ -MAA and $^{90\text{Y}}$ -microspheres and to improve lung shunt quantification (38).

Because selective treatments are advocated to avoid extrahepatic deposition of activity, the prescribed activity needs to be split according to target volumes. A simple one-third (left lobe) and two-thirds (right lobe) split is used by some centers, but most centers use the pretreatment CT scan for splitting the prescribed activity according to their manual liver segmentation. The most accurate method was proposed by Kao et al., who split the dose according to artery-specific SPECT/CT-based liver segmentation, delineating an artery-specific target volume based on $^{99\text{m}}\text{Tc}$ -MAA distribution (37). C-arm cone-beam CT may also be used for that particular goal.

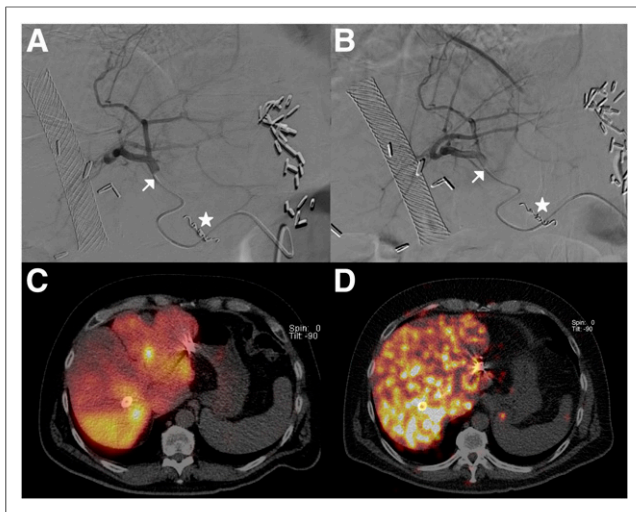


FIGURE 2. Patient with HCC recurrence in segment 7, who had previously undergone primary segmental resection with curative intent, cholecystectomy, and biliary stent placement. Gastroduodenal artery was coil-embolized (stars). Injection position is in left hepatic artery for ^{99m}Tc -MAA (A) and ^{90}Y -resin microspheres (B) (subsequent injection position in right hepatic artery not shown). Discrepancy of distribution between ^{99m}Tc -MAA SPECT/CT (C) and ^{90}Y PET/CT (D) can be acknowledged, with distribution in segment 4 being underestimated by ^{99m}Tc -MAA. These differences occurred even though the same 2-dimensional injection position was used in both angiographic procedures (arrows). Possible causes are the randomly shaped ^{99m}Tc -MAA vs. spheric microspheres, bolus injection ^{99m}Tc -MAA vs. intermittent injection ^{90}Y -microspheres, in-plane (3-dimensional) catheter tip position differences, and different numbers of particles injected during scout dose, inducing differences in flow dynamics.

TREATMENT

During administration of resin microspheres, stasis of blood flow may occur, leading to incomplete injection of all intended microspheres. Stasis is caused by an embolic effect due to the higher number of resin microspheres (30–50 million) than of glass microspheres (4 million). The specific activity of resin microspheres (50 kBq/sphere) is approximately 50 times lower than that of glass microspheres (2,500 kBq/sphere), but this may vary by shelf-life. Although resin microspheres have a stable specific activity during a 24-h shelf-life, the specific activity (and number of microspheres) may vary for glass microspheres, having a maximum 2-wk shelf-life. It has been postulated that a more heterogeneous distribution of glass microspheres leads to a preferable toxicity profile but that, vice versa, a more homogeneous distribution of resin microspheres may lead to a preferable efficacy profile (45). The Northwestern University group in Chicago therefore advocated the use of so-called extended shelf-life glass microspheres (46). Microsphere characteristics are important to consider when analyzing dose–response relationships. It is not fully understood whether the antitumor effect is merely a radiation effect or a combination of an ischemic and radiation effect, especially in the case of resin microspheres. The embolic effect of resin microspheres sometimes leads to acute ischemic pain during injection. Recently, however, it was shown that when 5% glucose is used instead of sterile water for injection, there is less pain, less stasis, and more efficient administration. The flow dynamics during administration will be an important research topic in the coming years. Flow dynamics influence tumor targeting and the predictive value of a scout dose for dose distribution and treatment planning.

POSTTREATMENT IMAGING AND DOSIMETRY

Initially, ^{90}Y -bremsstrahlung SPECT/CT was used after radioembolization to exclude extrahepatic activity deposition and to assess intrahepatic microsphere distribution. With 32 positrons per million decays, ^{90}Y PET/CT imaging has gradually taken over ^{90}Y -bremsstrahlung SPECT/CT, mainly because of new PET/CT scanners with time-of-flight technology. It allows more accurate quantification and dosimetry (47–49). Calculating tumor dose on posttreatment imaging may predict response (50–53). However, evidence was obtained in heterogeneous or small cohorts, mainly in HCC. Furthermore, the available studies differ in applied activity calculation method, used response criteria, and type of microsphere administered. Posttreatment imaging allows for detection of a heterogenic distribution of microspheres in the liver and in tumors, which correlates with partial or regional tumor response (49–51). In theory, after assessment of these parameters, additional radioembolization may be considered at an early stage, such as directly after administration of the treatment dose. However, the safety of repeated whole-liver radioembolization has not been firmly established yet (54,55).

Unfortunately, the true definition of the minimal effective tumor dose (and the maximum tolerated nontumor dose) remains a challenge. The reported tumor dose thresholds were found to be independent predictors of tumor response and survival, but lesion-based analyses on posttreatment imaging show that these numbers range widely (50,53). In a follow-up study of 56 HCC patients with 98 tumors, including a quantitative assessment on ^{90}Y PET/CT after radioembolization with glass microspheres, lesion-based analysis yielded a mean tumor dose of 215 Gy (range, 17–555 Gy) in responders, defined as partial or complete response according to modified Response Evaluation Criteria in Solid Tumors (mRECIST), and a mean tumor dose of 167 Gy (range, 35–465 Gy) in nonresponders (53). The true minimal effective tumor dose remains unknown and needs to be further investigated for each tumor type, tumor size, and microsphere type used.

Besides tumor dosimetry, ^{90}Y PET/CT allows early assessment of absorbed dose to healthy liver parenchyma: nontumor dose. At present, a nontumor dose of less than 70 Gy, or less than 50 Gy in cirrhotic livers, is assumed to be safe by the resin microsphere manufacturer (33). Nonetheless, a nontumor dose above these limits has been described. Using pretreatment dosimetry, a nontumor dose of less than 120 Gy on treatment planning was accepted for glass microspheres without additional toxicities (8). Like tumor dose, the maximum tolerated nontumor dose needs to be refined for baseline liver function, treatment history, tumor characteristics, and type of microsphere used.

CLINICAL OUTCOME AND TUMOR RESPONSE

In general, radioembolization is well tolerated. Mild clinical side effects usually occur within 4–6 wk after radioembolization (e.g., abdominal pain, nausea, vomiting, fatigue, and fever) (2). More serious complications (1–3 mo after radioembolization) include complications due to extrahepatic deposition of activity (e.g., gastric ulceration, pancreatitis, radiation pneumonitis) and liver decompensation. Excessive irradiation of healthy liver parenchyma leads to the most serious and life-threatening complication after radioembolization: radioembolization-induced liver disease. This is thought to be a venoocclusive disease/sinusoidal obstruction syndrome (56). Extensive sinusoidal congestion was acknowledged in liver biopsies, affecting the perivenular spaces with hepatic atrophy and necrosis

TABLE 5
Landmark Studies on Response and Survival in Liver Malignancies

Study	Design	Tumor	Treatment	Patients (n)	Response criteria	CR (%)	PR (%)	SD (%)	PD (%)	TTHP (mo)	MS (mo)
Kolligs (60)	Pilot randomized controlled trial	HCC; BCLC A–C; Child–Pugh ≤ B7	RE	13	RECIST 1.0	0	30.8	46.2	15.4	3.7	NA
			CE	15		0	13.3	60.0	20.0	3.6	NA
Gramenzi (62)	Single-center, prospective cohort	HCC; BCLC B–C; Child–Pugh ≤ B7	RE	63	mRECIST	14.3	53.9	14.3	17.5	3	13.2
			Sorafenib	73		62.5		18.8	18.7	3	11.2
						0	9.5	41.9	48.6	5	14.4
						9.4		37.5	53.1	3	13.1
Al-Adra (72)	Systematic review	Intrahepatic cholangiocarcinoma	RE	298	Pooled analysis	0	28	54	18	NA	15.5
Devic (77)	Metaanalysis	Neuroendocrine tumor	RE	435	Pooled analysis	50		36	14	NA	28.5
Saxena (67)	Systematic review	Metastatic colorectal cancer	RE	979	Pooled analysis	0	31	40.5	17.5	9	12

CR = complete response; PR = partial response; SD = stable disease; PD = progressive disease; TTHP = median time to hepatic progression; MS = median survival; RE = radioembolization; NA = not available; CE = chemoembolization.

Italicized numbers are confounder-corrected results. Boldface numbers are data for CR and PR combined.

around portal veins with fresh thrombus. In an early stage after radioembolization, serum markers show an induction of oxidative stress. Simultaneously, proinflammatory pathways are activated, resulting in endothelial injury with the activation of the coagulation cascade (57). Jaundice and ascites, in the absence of tumor progression or bile duct dilatation, are the main symptoms of radioembolization-induced liver disease (56,58). General risk factors for developing radioembolization-induced liver disease include prior chemotherapy, low tumor burden, high baseline bilirubin values, and cirrhotic liver disease (56,58).

Table 5 features the efficacy results of several landmark studies in the field of radioembolization.

In the intermediate and early-advanced stages of HCC (respectively, BCLC B and BCLC C), radioembolization has shown favorable outcomes compared with the currently preferred treatments (59,60). Compared with TACE, radioembolization has a similar or even better objective response rate and similar survival statistics (60). Moreover, as previously discussed, PVT and bili-digestive anastomoses are no absolute contraindication. Additionally, an ECOG performance score of at least 1 and a large tumor size (>10 cm) are currently considered a contraindication for TACE, in contrast to radioembolization (ECOG performance score ≤ 2, no tumor size limitation) (61). Radioembolization seems to effectively reduce the size of large tumors (Fig. 3), and response rates of up to 91% have been described (8).

In BCLC B or BCLC C, not suitable for TACE, the current recommendation is systemic treatment with the multikinase inhibitor sorafenib. However, these patients might benefit more from radioembolization than from sorafenib. Recently, a large study (62) showed significantly better response rates and fewer adverse events after radioembolization than after sorafenib, even after correction of confounders (Table 5); survival was similar. Patients are currently being recruited for the YES-P, SARAH, and SIRVENIB trials, in which sorafenib and radioembolization

will be compared in a randomized controlled setting. The results of a phase II study in the Asia-Pacific trial indicate that combining both treatments seems beneficial, with manageable toxicities (63). This is currently under investigation in the SORAMIC trial (resin microspheres) and the STOP-HCC trial (glass microspheres). Patients who are ineligible or poor candidates for TACE are randomized into 2 groups: a group receiving sorafenib combined with radioembolization and a group receiving sorafenib alone. Even though radioembolization is currently not incorporated into the BCLC scheme and the results of the above-mentioned trials are pending, for selected patients radioembolization can be positioned between TACE and sorafenib (Fig. 4).

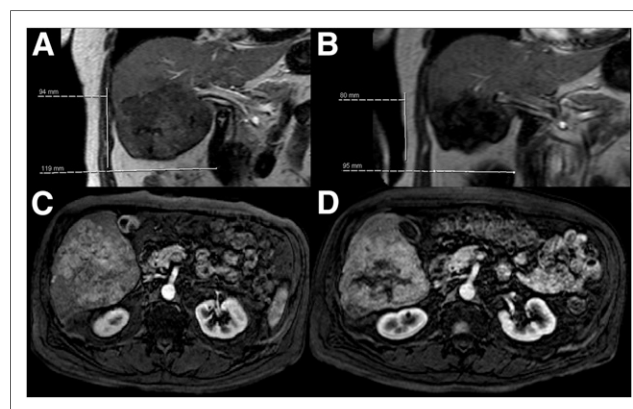


FIGURE 3. Patient with large HCC (12 cm) in right lobe on T1-weighted MR imaging sequences in coronal plane: before radioembolization (A); tumor shrinkage after radioembolization (B); T1-weighted gadolinium-enhanced MR image with fat suppression in axial plane during arterial phase (20 s after injection), illustrating hypervascular tumor (C); large area of necrosis in tumor on same sequence after radioembolization (D).

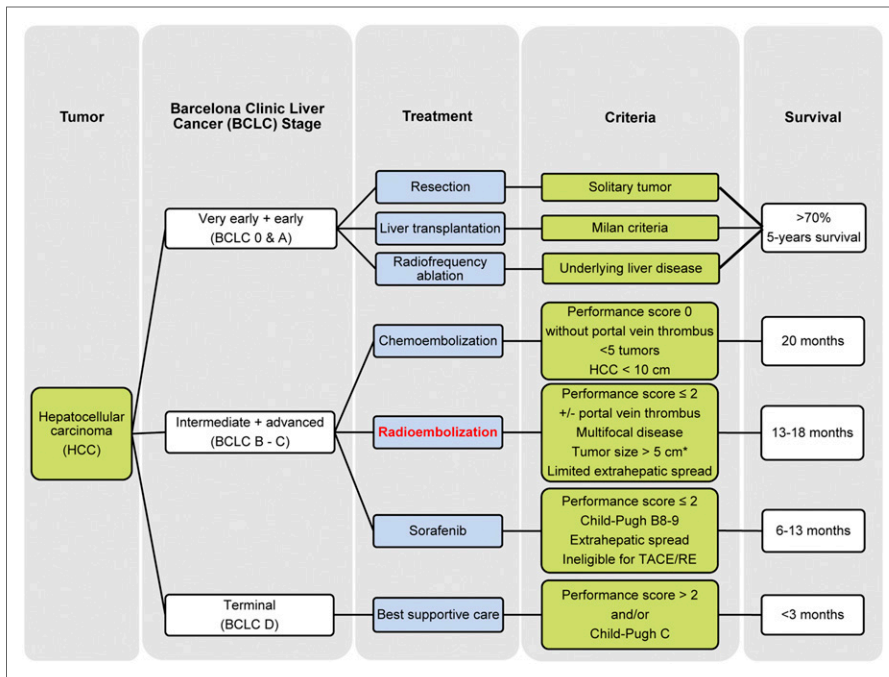


FIGURE 4. BCLC staging system with proposal for radioembolization in treatment paradigm. Because the applicability of radioembolization in intermediate- and advanced-stage HCC overlaps, these stages have been combined in this proposal. *Size of tumors has been included in this BCLC scheme; however, exact size limits need to be investigated further.

In patients with focal or limited disease, ineligible for surgical resection or radiofrequency ablation, radioembolization using glass microspheres may provide an interesting alternative: radiation segmentectomy is meant to provide an ablating radiation dose (>200 Gy) by selective or superselective catheterization. By selective target-

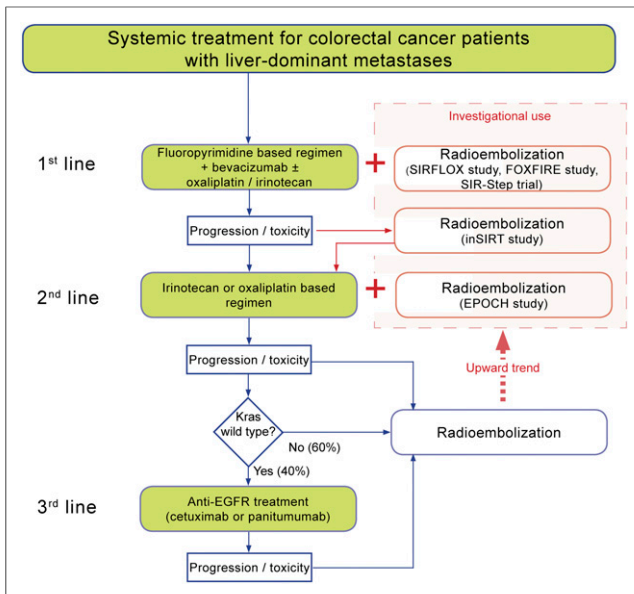


FIGURE 5. Schematic of evolving application of radioembolization in metastatic colorectal cancer and current trials. At present, radioembolization is applied mainly in the salvage setting; however, many clinical trials focus on bringing radioembolization to the forefront of the metastatic colorectal cancer treatment algorithm in the first- or second-line setting.

ing, necrosis is induced in a limited portion of the liver, including the tumor, thus sparing radiation to healthy liver parenchyma. Vouche et al. described a high objective response rate (88%) and median overall survival (53.4 mo) using this technique in solitary HCCs smaller than 5 cm (64). In their cohort, 33% of patients were amenable to liver transplantation after radiation segmentectomy. At pathologic examination of the native liver specimens, 100% necrosis and more than 90% necrosis were found in, respectively, 52% and 48% of patients (64). In HCC, the downstaging success rate with radioembolization is around 50% (range, 29%–67%), with a median time to downstaging of 3.1–4 mo (65). In downstaging HCC, radioembolization is a suitable alternative to TACE, but downstaging should not be restricted to HCC alone (65).

The current European Society for Medical Oncology guideline on metastatic colorectal cancer states that in patients with liver-limited disease and unresectable liver metastases failing available chemotherapeutic regimens, radioembolization using resin microspheres prolongs time to tumor progression (66). Results in heavily pretreated patients with chemoresistant metastatic colorectal cancer have been consistent over the years, making salvage treatment with radioembolization a widely accepted indication. According to a recent systematic review, treated patients have failed a median of 3 chemotherapeutic regimens before radioembolization (67). Left untreated, patients with chemorefractory liver metastases have a median survival of only 5–7 mo (68–70). Nonetheless, in this population with an overall poor prognosis, after radioembolization a mean objective response rate of 31%, median progression-free survival of 9 mo, and median overall survival of 12 mo are obtained (Table 5) (67). Several ongoing randomized controlled trials are establishing the role of radioembolization for metastatic colorectal cancer (Fig. 5). The addition of radioembolization to first-line chemotherapy regimens is being investigated in the SIRFLOX, FOXFIRE, and SIR-step trials (all using resin microspheres). After first-line failure, the EPOCH trial will randomize patients in second-line chemotherapy with or without radioembolization (glass microspheres).

Another relatively new application of radioembolization before surgical resection is the induction of hypertrophy of the contralateral lobe by radioembolization of the diseased lobe. After portal vein embolization, 17.5% of patients are ineligible for surgical resection because of tumor progression, and in 4.8% of patients, hypertrophy induction of the future liver remnant is insufficient (71). Compared with portal vein embolization, induction of hypertrophy by radioembolization is similar but takes longer. A degree of hypertrophy of approximately 35% (8.9%–57%) can be obtained in 3–4 mo (65). Theoretically, the main benefit of radioembolization is simultaneous tumor treatment, reducing the number of dropouts due to disease progression.

Unresectable intrahepatic cholangiocarcinoma, left untreated, has an overall survival of less than 8 mo, and with gemcitabine

and cisplatin overall survival is 11.7 mo (72,73). After radioembolization, overall survival of 15.5 mo can be reached (72). Repeated radioembolization can lead to local disease control for a longer period (Supplemental Fig. 1; supplemental materials are available at <http://jnm.snmjournals.org>). Radioembolization before surgical resection, as in HCC and metastatic colorectal cancer, could be promising in intrahepatic cholangiocarcinoma as well. Downstaging occurs in 10%, and inducing contralateral hypertrophy seems feasible (65,72). In a small cohort combining radioembolization with chemotherapy, downstaging occurred in 22%, significant hypertrophy of the contralateral lobes was seen in all patients, and 18% were radically resected (74). In general, these results for intrahepatic cholangiocarcinoma are promising, but current literature is limited.

The heterogeneous group of neuroendocrine tumors has a lower incidence than the aforementioned tumors, though hepatic involvement in neuroendocrine tumors is common and is the greatest incriminating factor in survival (disease-free survival, 20 mo with >4 hepatic metastases, vs. 46 mo with ≤4 hepatic metastases) (75). Most patients present with multifocal hepatic disease and are ineligible for resection or radiofrequency ablation (76). Conventional treatments (i.e., somatostatin analogs) and newer biologicals (i.e., sunitinib and everolimus) improve survival, but the objective response rate is poor. Because of the hypervascular nature of hepatic metastases, neuroendocrine tumors are prime candidates for radioembolization. In a metaanalysis including 414 patients, the pooled objective response rate was 50%, disease control rate was 86%, and overall survival was 28.5 mo (Table 5) (77). Data reporting response rates based on the primary tumor origin and according to the World Health Organization histologic grading system are needed.

CONCLUSION

Hepatic ⁹⁰Y radioembolization continues to develop rapidly. Clinical research is expanding indications in many different tumor types, overcoming technical angiographic challenges, fine-tuning the application of dosimetry, and optimizing quantitative imaging in daily practice.

REFERENCES

- Sangro B, Salem R, Kennedy A, Coldwell D, Wasan H. Radioembolization for hepatocellular carcinoma: a review of the evidence and treatment recommendations. *Am J Clin Oncol*. 2011;34:422–431.
- Kennedy A, Nag S, Salem R, et al. Recommendations for radioembolization of hepatic malignancies using yttrium-90 microsphere brachytherapy: a consensus panel report from the radioembolization brachytherapy oncology consortium. *Int J Radiat Oncol Biol Phys*. 2007;68:13–23.
- Golfieri R, Bilbao JI, Carpanese L. Comparison of the survival and tolerability of radioembolization in elderly vs. younger patients with unresectable hepatocellular carcinoma. *J Hepatol*. 2013;59:753–761.
- Tohme S, Sukato D, Nace GW, et al. Survival and tolerability of liver radioembolization: a comparison of elderly and younger patients with metastatic colorectal cancer. *HPB (Oxford)*. 2014;16:1110–1116.
- Patel NH, Sasadeusz KJ, Seshadri R, et al. Increase in hepatic arterial blood flow after transjugular intrahepatic portosystemic shunt creation and its potential predictive value of postprocedural encephalopathy and mortality. *J Vasc Interv Radiol*. 2001;12:1279–1284.
- Sato K, Lewandowski RJ, Bui JT. Treatment of unresectable primary and metastatic liver cancer with yttrium-90 microspheres (TheraSphere): assessment of hepatic arterial embolization. *Cardiovasc Intervent Radiol*. 2006;29:522–529.
- Goin JE, Roberts CA, Dancy JE, Sickles CJ, Leung DA, Soulen MC. Comparison of post-embolization syndrome in the treatment of patients with unresectable hepatocellular carcinoma: trans-catheter arterial chemo-embolization versus yttrium-90 glass microspheres. *World J Nucl Med*. 2004;3:49–56.
- Garin E, Rolland Y, Edeline J, et al. Personalized dosimetry and intensification concept with ⁹⁰Y-loaded glass microsphere radioembolization induce prolonged overall survival in hepatocellular carcinoma patients with portal vein thrombosis. *J Nucl Med*. 2015;56:339–346.
- Salem R, Lewandowski RJ, Mulcahy MF, et al. Radioembolization for hepatocellular carcinoma using yttrium-90 microspheres: a comprehensive report of long-term outcomes. *Gastroenterology*. 2010;138:52–64.
- Mazzaferro V, Sposito C, Bhoori S. Yttrium-90 radioembolization for intermediate-advanced hepatocellular carcinoma: a phase 2 study. *Hepatology*. 2013;57:1826–1837.
- Shi J, Lai EC, Li N, et al. Surgical treatment of hepatocellular carcinoma with portal vein tumor thrombus. *Ann Surg Oncol*. 2010;17:2073–2080.
- Kulik LM, Carr BI, Mulcahy MF, et al. Safety and efficacy of ⁹⁰Y radiotherapy for hepatocellular carcinoma with and without portal vein thrombosis. *Hepatology*. 2008;47:71–81.
- Atassi B, Bangash AK, Lewandowski RJ, et al. Biliary sequelae following radioembolization with yttrium-90 microspheres. *J Vasc Interv Radiol*. 2008;19:691–697.
- Kim W, Clark TW, Baum RA, Soulen MC. Risk factors for liver abscess formation after hepatic chemoembolization. *J Vasc Interv Radiol*. 2001;12:965–968.
- Woo S, Chung JW, Hur S, et al. Liver abscess after transarterial chemoembolization in patients with bilioenteric anastomosis: frequency and risk factors. *AJR*. 2013;200:1370–1377.
- Geisel D, Powerski MJ, Schnapauff D. No infectious hepatic complications following radioembolization with ⁹⁰Y microspheres in patients with biliodigestive anastomosis. *Anticancer Res*. 2014;34:4315–4321.
- Cholapranee A, van Houten D, Deitrick G, et al. Risk of liver abscess formation in patients with prior biliary intervention following yttrium-90 radioembolization. *Cardiovasc Intervent Radiol*. 2015;38:397–400.
- Mascarenhas N, Ryu RK, Salem R. Hepatic radioembolization complicated by abscess. *Semin Intervent Radiol*. 2011;28:222–225.
- van den Hoven AF, Smits MLJ, de Keizer B, et al. Identifying aberrant hepatic arteries prior to intra-arterial radioembolization. *Cardiovasc Intervent Radiol*. 2014;37:1482–1493.
- Powerski MJ, Erxleben C, Scheurig-Münkler C, et al. Anatomic variants of arteries often coil-occluded prior to hepatic radioembolization. *Acta Radiol*. 2015;56:159–165.
- Vesselle G, Petit I, Boucebei S, Rocher T, Velasco S, Tasu JP. Radioembolization with yttrium-90 microspheres work up: practical approach and literature review. *Diagn Interv Imaging*. April 25, 2014 [Epub ahead of print].
- Abdelmaksoud MH, Hwang GL, Louie JD, et al. Development of new hepatic-arteric collateral pathways after hepatic arterial skeletonization in preparation for yttrium-90 radioembolization. *J Vasc Interv Radiol*. 2010;21:1385–1395.
- Hamoui N, Minocha J, Memon K, et al. Prophylactic embolization of the gastroduodenal and right gastric arteries is not routinely necessary before radioembolization with glass microspheres. *J Vasc Interv Radiol*. 2013;24:1743–1745.
- Lam MGEH, Banerjee S, Louie JD, et al. Root cause analysis of gastroduodenal ulceration after yttrium-90 radioembolization. *Cardiovasc Intervent Radiol*. 2013;36:1536–1547.
- Barentsz MW, Vente MAD, Lam MGEH, et al. Technical solutions to ensure safe yttrium-90 radioembolization in patients with initial extrahepatic deposition of ^{90m}technetium-albumin macroaggregates. *Cardiovasc Intervent Radiol*. 2011;34:1074–1079.
- Dudeck O, Wilhelmsen S, Ulrich G, et al. Effectiveness of repeat angiographic assessment in patients designated for radioembolization using yttrium-90 microspheres with initial extrahepatic accumulation of technetium-99m macroaggregated albumin: a single center's experience. *Cardiovasc Intervent Radiol*. 2012;35:1083–1093.
- Liu D, Cade D, Worsley D, Klass D, Lim H, Arepally A. Single procedure yttrium-90 (SPY90): pilot study of a consolidated single procedure selective internal radiation therapy without prior-MAA nuclear medicine scan or prophylactic embolization utilizing yttrium-90 resin microspheres [abstract]. *Cardiovasc Intervent Radiol*. 2013;36(3, suppl)S321.
- Louie JD, Kothary N, Kuo WT, et al. Incorporating cone-beam CT into the treatment planning for yttrium-90 radioembolization. *J Vasc Interv Radiol*. 2009;20:606–613.
- Wright CL, Werner JD, Tran JM, et al. Radiation pneumonitis following yttrium-90 radioembolization: case report and literature review. *J Vasc Interv Radiol*. 2012;23:669–674.
- Leung TW, Lau WY, Ho SK. Radiation pneumonitis after selective internal radiation treatment with intraarterial ⁹⁰yttrium-microspheres for inoperable hepatic tumors. *Int J Radiat Oncol Biol Phys*. 1995;33:919–924.
- Yu N, Srinivas SM, Difilippo FP, et al. Lung dose calculation with SPECT/CT for ⁹⁰yttrium radioembolization of liver cancer. *Int J Radiat Oncol Biol Phys*. 2013;85:834–839.

32. Elschot M, Nijssen JFW, Lam MGEH, et al. ^{99m}Tc -MAA overestimates the absorbed dose to the lungs in radioembolization: a quantitative evaluation in patients treated with ^{166}Ho -microspheres. *Eur J Nucl Med Mol Imaging*. 2014;41:1965–1975.
33. SIR-spheres[®] microspheres package insert. SirTex website. <http://www.sirtex.com/media/29845/ssl-us-10.pdf>. Published November 2014. Accessed May 7, 2015.
34. TheraSphere[®] yttrium-90 glass microspheres. TheraSphere website. http://www.thersphere.com/physicians-package-insert/TS_PackageInsert_USA_v12.pdf. Accessed May 7, 2015.
35. Lam MGEH, Louie JD, Abdelmaksoud MH, Fisher GA, Cho-Phan CD, Sze DY. Limitations of body surface area-based activity calculation for radioembolization of hepatic metastases in colorectal cancer. *J Vasc Interv Radiol*. 2014;25:1085–1093.
36. Kao YH, Tan EH, Ng CE, Goh SW. Clinical implications of the body surface area method versus partition model dosimetry for yttrium-90 radioembolization using resin microspheres: a technical review. *Ann Nucl Med*. 2011;25:455–461.
37. Kao YH, Hock Tan AE, Burgmans MC, et al. Image-guided personalized predictive dosimetry by artery-specific SPECT/CT partition modeling for safe and effective ^{90}Y radioembolization. *J Nucl Med*. 2012;53:559–566.
38. Smits MLJ, Elschot M, Sze DY, et al. Radioembolization dosimetry: the road ahead. *Cardiovasc Intervent Radiol*. 2015;38:261–269.
39. Flamen P, Vanderlinden B, Delatte P. Multimodality imaging can predict the metabolic response of unresectable colorectal liver metastases to radioembolization therapy with yttrium-90 labeled resin microspheres. *Phys Med Biol*. 2008;53:6591–6603.
40. Garin E, Lenoir L, Rolland Y, et al. Dosimetry based on ^{99m}Tc -macroaggregated albumin SPECT/CT accurately predicts tumor response and survival in hepatocellular carcinoma patients treated with ^{90}Y -loaded glass microspheres: preliminary results. *J Nucl Med*. 2012;53:255–263.
41. Strigari L, Sciuto R, Rea S, et al. Efficacy and toxicity related to treatment of hepatocellular carcinoma with ^{90}Y -SIR spheres: radiobiologic considerations. *J Nucl Med*. 2010;51:1377–1385.
42. Campbell JM, Wong CO, Muzik O, et al. Early dose response to yttrium-90 microsphere treatment of metastatic liver cancer by a patient-specific method using single photon emission computed tomography and positron emission tomography. *Int J Radiat Oncol Biol Phys*. 2009;74:313–320.
43. Cremonesi M, Chiesa C, Strigari L, et al. Radioembolization of hepatic lesions from a radiobiology and dosimetric perspective. *Front Oncol*. 2014;4:210.
44. Eaton BR, Kim HS, Schreiber E, et al. Quantitative dosimetry for yttrium-90 radionuclide therapy: tumor dose predicts fluorodeoxyglucose positron emission tomography response in hepatic metastatic melanoma. *J Vasc Interv Radiol*. 2014;25:288–295.
45. Walrand S, Hesse M, Chiesa C, Lhommel R, Jamar F. The low hepatic toxicity per gray of ^{90}Y glass microspheres is linked to their transport in the arterial tree favoring a nonuniform trapping as observed in posttherapy PET imaging. *J Nucl Med*. 2014;55:135–140.
46. Lewandowski RJ, Minocha J, Memon K, et al. Sustained safety and efficacy of extended-shelf-life ^{90}Y glass microspheres: long-term follow-up in a 134-patient cohort. *Eur J Nucl Med Mol Imaging*. 2014;41:486–493.
47. Elschot M, Vermolen BJ, Lam MGEH, et al. Quantitative comparison of PET and bremsstrahlung SPECT for imaging the in vivo yttrium-90 microsphere distribution after liver radioembolization. *PLoS ONE*. 2013;8:e55742.
48. Zade AA, Rangarajan V, Purandare NC, et al. ^{90}Y microsphere therapy: does ^{90}Y PET/CT imaging obviate the need for ^{90}Y bremsstrahlung SPECT/CT imaging? *Nucl Med Commun*. 2013;34:1090–1096.
49. Kao YH, Steinberg JD, Tay YS, et al. Post-radioembolization yttrium-90 PET/CT: part 1—diagnostic reporting. *EJNMMI Res*. 2013;3:56.
50. Kao YH, Steinberg JD, Tay YS, et al. Post-radioembolization yttrium-90 PET/CT: part 2—dose-response and tumor predictive dosimetry for resin microspheres. *EJNMMI Res*. 2013;3:57.
51. Padia SA, Alessio A, Kwan SW, et al. Comparison of positron emission tomography and bremsstrahlung imaging to detect particle distribution in patients undergoing yttrium-90 radioembolization for large hepatocellular carcinomas or associated portal vein thrombosis. *J Vasc Interv Radiol*. 2013;24:1147–1153.
52. D'Arienzo M, Chiaromida P, Chiacchiararelli L, et al. ^{90}Y PET-based dosimetry after selective internal radiotherapy treatments. *Nucl Med Commun*. 2012;33:633–640.
53. Srinivas SM, Natarajan N, Kuroiwa J, et al. Determination of radiation absorbed dose to primary liver tumors and normal liver tissue using post-radioembolization ^{90}Y PET. *Front Oncol*. 2014;4:255.
54. Zarva A, Mohnike K, Damm R, et al. Safety of repeated radioembolizations in patients with advanced primary and secondary liver tumors and progressive disease after first selective internal radiotherapy. *J Nucl Med*. 2014;55:360–366.
55. Lam MGEH, Louie JD, Iagaru AH, Goris ML, Sze DY. Safety of repeated yttrium-90 radioembolization. *Cardiovasc Intervent Radiol*. 2013;36:1320–1328.
56. Sangro B, Gil-Alzugaray B, Rodriguez J, et al. Liver disease induced by radioembolization of liver tumors: description and possible risk factors. *Cancer*. 2008;112:1538–1546.
57. Fernandez-Ros N, Iñarrairaegui M, Paramo JA, et al. Radioembolization of hepatocellular carcinoma activates liver regeneration, induces inflammation and endothelial stress and activates coagulation. *Liver Int*. 2015;35:1590–1596.
58. Gil-Alzugaray B, Chopitea A, Iñarrairaegui M, et al. Prognostic factors and prevention of radioembolization-induced liver disease. *Hepatology*. 2013;57:1078–1087.
59. Colombo M, Sangiovanni A. Treatment of hepatocellular carcinoma: beyond international guidelines. *Liver Int*. 2015;35(suppl 1):129–138.
60. Kolligs FT, Bilbao JI, Jakobs T, et al. Pilot randomized trial of selective internal radiation therapy vs. chemoembolization in unresectable hepatocellular carcinoma. *Liver Int*. November 29, 2014 [Epub ahead of print].
61. Raulo JL, Sangro B, Forner A, et al. Evolving strategies for the management of intermediate-stage hepatocellular carcinoma: available evidence and expert opinion on the use of transarterial chemoembolization. *Cancer Treat Rev*. 2011;37:212–220.
62. Granzen A, Gölfieri R, Mosconi C, et al. Yttrium-90 radioembolization vs sorafenib for intermediate-locally advanced hepatocellular carcinoma: a cohort study with propensity score analysis. *Liver Int*. 2015;35:1036–1047.
63. Chow PK, Poon DY, Khin MW, et al. Multicenter phase II study of sequential radioembolization-sorafenib therapy for inoperable hepatocellular carcinoma. *PLoS ONE*. 2014;9:e90909.
64. Vouche M, Habib A, Ward TJ, et al. Unresectable solitary hepatocellular carcinoma not amenable to radiofrequency ablation: multicenter radiology-pathology correlation and survival of radiation segmentectomy. *Hepatology*. 2014;60:192–201.
65. Braat AJAT, Huijbregts JE, Molenaar IQ, et al. Hepatic radioembolization as a bridge to liver surgery. *Front Oncol*. 2014;4:199.
66. Van Cutsem E, Cervantes A, Nordlinger B, et al. Metastatic colorectal cancer: ESMO clinical practice guidelines for diagnosis, treatment and follow-up. *Ann Oncol*. 2014;25(suppl 3):iii1–iii9.
67. Saxena A, Bester L, Shan L, et al. A systematic review on the safety and efficacy of yttrium-90 radioembolization for unresectable, chemorefractory colorectal cancer liver metastases. *J Cancer Res Clin Oncol*. 2014;140:537–547.
68. Lemmens VE, de Haan N, Rutten HJ, et al. Improvements in population-based survival of patients presenting with metastatic rectal cancer in the south of the Netherlands, 1992–2008. *Clin Exp Metastasis*. 2011;28:283–290.
69. Meulenbeld HJ, van Steenberg LN, Janssen-Heijnen ML, et al. Significant improvement in survival of patients presenting with metastatic colon cancer in the south of The Netherlands from 1990 to 2004. *Ann Oncol*. 2008;19:1600–1604.
70. Welch S, Spithoff K, Rumble RB, et al. Bevacizumab combined with chemotherapy for patients with advanced colorectal cancer: a systematic review. *Ann Oncol*. 2010;21:1152–1162.
71. Vyas S, Markar S, Partelli S, et al. Portal vein embolization and ligation for extended hepatectomy. *Indian J Surg Oncol*. 2014;5:30–42.
72. Al-Adra DP, Gill RS, Axford SJ, et al. Treatment of unresectable intrahepatic cholangiocarcinoma with yttrium-90 radioembolization: a systematic review and pooled analysis. *Eur J Surg Oncol*. 2015;41:120–127.
73. Brown KM, Parmar AD, Geller DA. Intrahepatic cholangiocarcinoma. *Surg Oncol Clin N Am*. 2014;23:231–246.
74. Rayar M, Sulpice L, Edeline J, et al. Intra-arterial yttrium-90 radioembolization combined with systemic chemotherapy is a promising method for downstaging huge intrahepatic cholangiocarcinoma to surgical treatment. *Ann Surg Oncol*. January 27, 2015 [Epub ahead of print].
75. Yao KA, Talamonti MS, Nemcek A, et al. Indications and results of liver resection and hepatic chemoembolization for metastatic gastrointestinal neuroendocrine tumors. *Surgery*. 2001;130:677–682.
76. Pavel M, Baudin E, Couvelard A, et al. ENETS consensus guidelines for the management of patients with liver and other distant metastases from neuroendocrine neoplasms of foregut, midgut, hindgut, and unknown primary. *Neuroendocrinology*. 2012;95:157–176.
77. Devic Z, Rosenberg J, Braat AJAT, et al. The efficacy of hepatic ^{90}Y resin radioembolization for metastatic neuroendocrine tumors: a meta-analysis. *J Nucl Med*. 2014;55:1404–1410.
78. Korkmaz M, Bozkaya H, Çınar C, et al. Liver abscess following radioembolization with yttrium-90 microspheres. *Wien Klin Wochenschr*. 2014;126:785–788.
79. Prince JF, van den Hoven AF, van den Bosch MAAJ, et al. Radiation-induced cholecystitis after hepatic radioembolization: do we need to take precautionary measures? *J Vasc Interv Radiol*. 2014;25:1717–1723.
80. Bilbao JI. Radioembolization and the cystic artery. *J Vasc Interv Radiol*. 2014;25:1724–1726.